



Clustering of simulated gravitational-wave signals from core-collapse supernovae using machine learning

Yusuke Sakai

Team: T. S. Yamamoto, T. Nishimura, Y. Terada, C. Allene, M. Meyer-Conde,
K. Sakai, K. Oohara, H. Takahashi

The 2nd AI+HEP in East Asia workshop @KEK, Jan 23, 2026



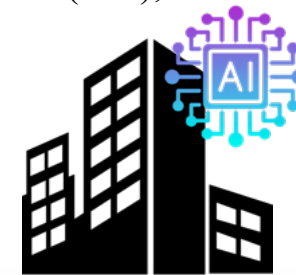
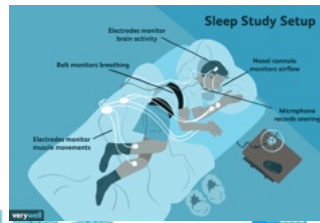
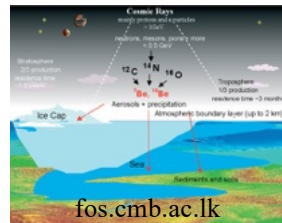
Self introduction 🙋

Yusuke Sakai / 坂井 佑輔

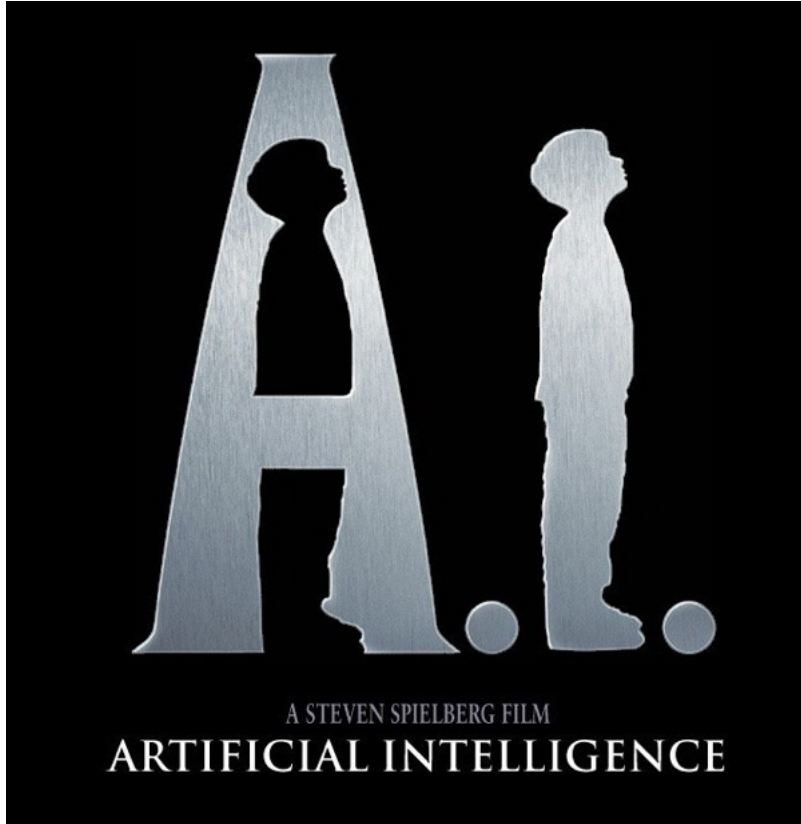


Year	
2019	Master of Science, <i>Niigata University</i>
2024	Ph.D. in Engineering, <i>Tokyo City University</i>
2024~ 2026	Postdoctoral Researcher, Research Center for Space Science, Tokyo City University

- Analysis Method
 - **Time-Frequency Analysis**: Digital Filtering, FFT, Wavelet Transform, Hilbert-Huang Transform
 - **Machine Learning**
 - Traditional model : SVM, KNN, k-means++, Spectral Clustering, t-SNE, UMAP
 - Deep Learning model: MLPs, CNN, VAE, LSTM, Transformer
- Application Domains
 - Gravitational-Wave, Cosmic Ray, Medical Science, Intelligent Transportation Systems (IST), Construction Analytics



Software Design for Machine Learning

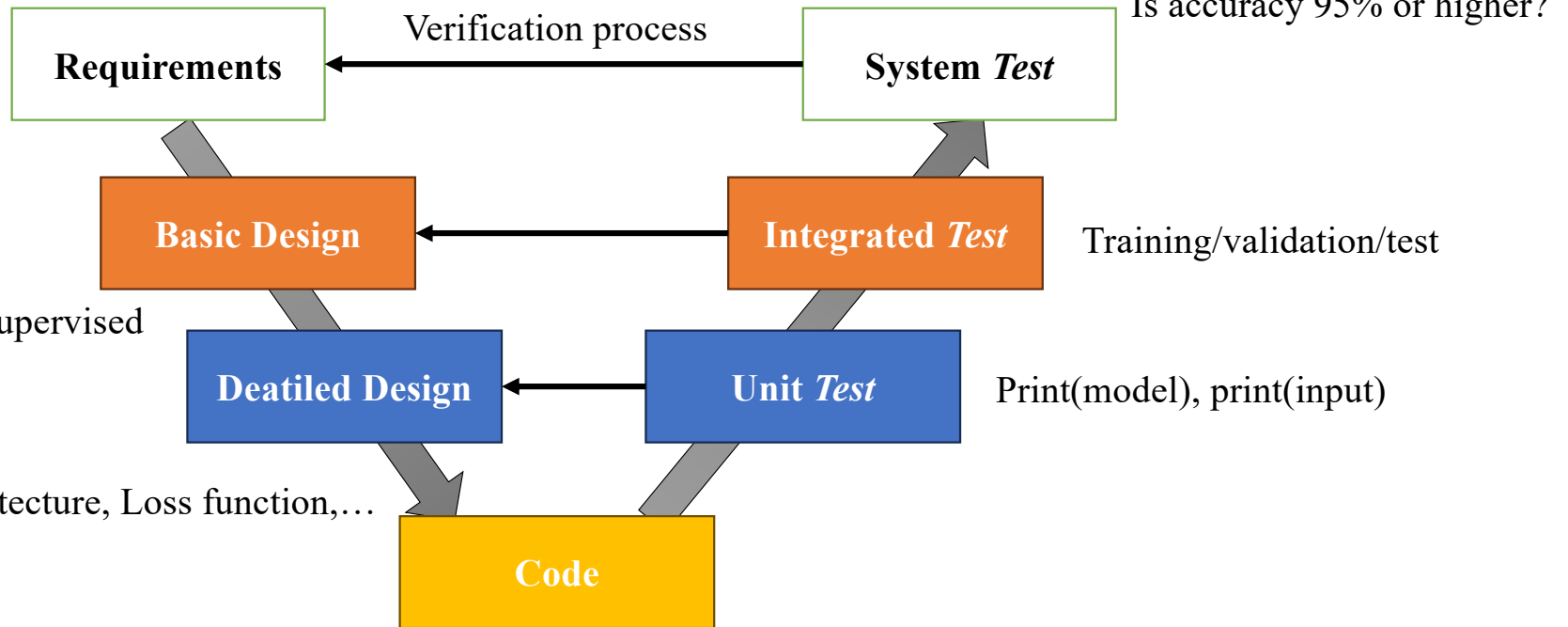


Gravitational-Wave Analysis from Supernova



Water-Fall Design (V-Model)

Accuacy 95% on MNIST



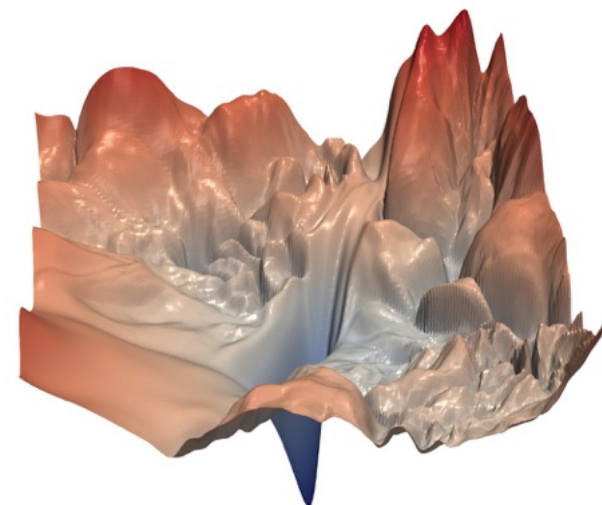
CNN, Preprocessing, Supervised

Optimizer, CNN architecture, Loss function,...

It might be difficult to confirm whether the training is appropriate...

To be confirmed items in the Integrated *test* phase are listed:

- Deep Learning Architecture: MLPs, Transformer, CNN, ...
- Optimizer: Adam, Sophia, ...
- Training Scheduler,
- Batch-size, Epochs, ...
- Scaling Law: Dataset size & Parameter numbers,
- Overfitting, Loss landscape

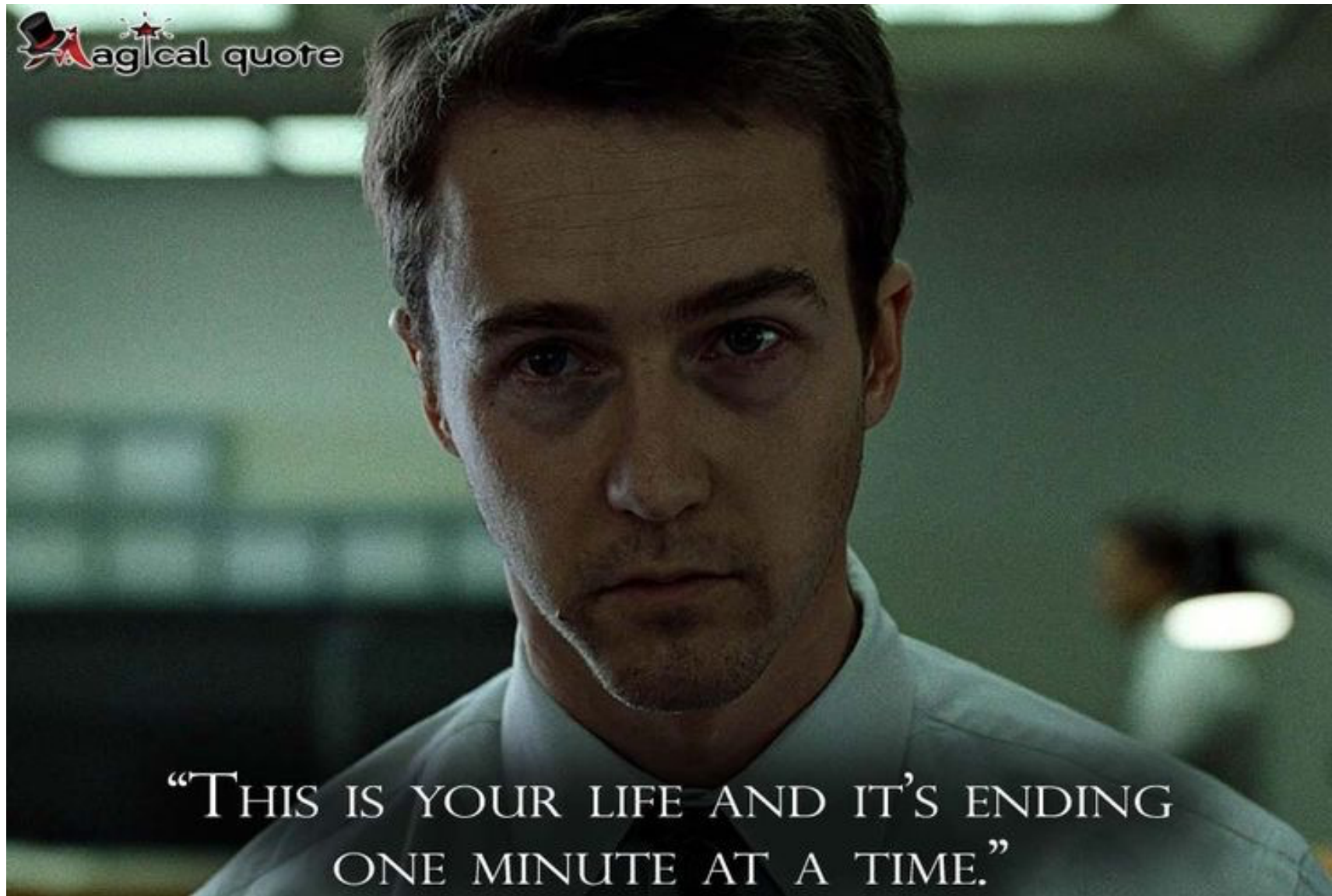


Visualizing the loss landscape of ResNet56 [1]

Since the verification items are dependent, learning optimization is not a simple task.

How much time can you achieve those complex task?

[1] LI, Hao, et al. Visualizing the loss landscape of neural nets. *Advances in neural information processing systems*, 2018, 31.



“THIS IS YOUR LIFE AND IT’S ENDING
ONE MINUTE AT A TIME.”

If your model tries to learn the traffic color from this image, it would fail.



Can we do better in terms of training optimization?



Data Analysis Workflow

Upstream stage

Data Acquisition



Preprocessing



Analysis (ML)



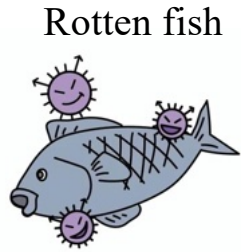
Evaluation

Downstream stage

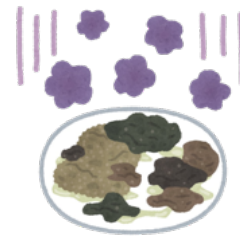
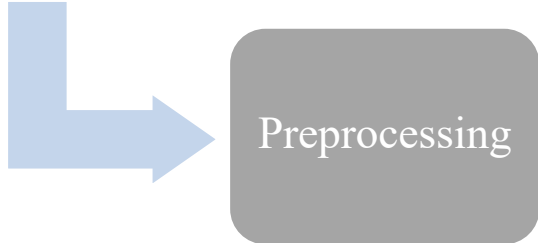


Data Analysis Workflow

Upstream stage



Even the best chef (AI) cannot create an excellent dish from rotten fish. This is why verification at the upstream stages is important!



Downstream stage

Effectiveness of Incorporating Frequency Information

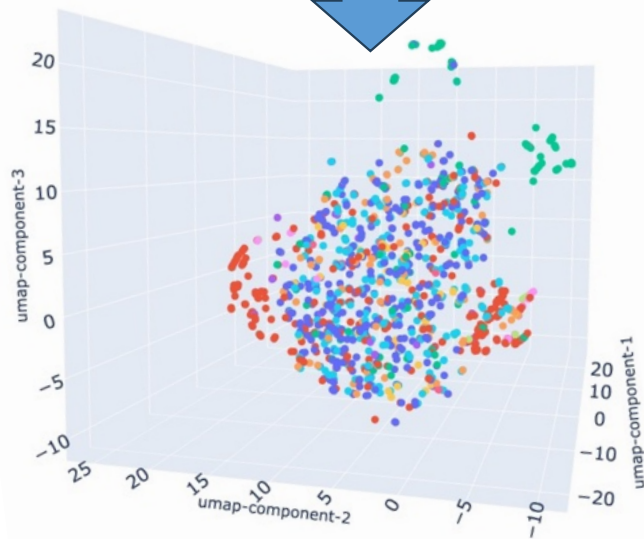
- YI, Kun, et al. A survey on deep learning based time series analysis with frequency transformation. In: *Proceedings of the 31st ACM SIGKDD Conference on Knowledge Discovery and Data Mining V. 2*. 2025. p. 6206-6215.
- YI, Kun, et al. Frequency-domain MLPs are more effective learners in time series forecasting. *Advances in Neural Information Processing Systems*, 2023, 36: 76656-76679.
- Ormiston, Rich, et al. "Noise reduction in gravitational-wave data via deep learning." *Physical Review Research* 2.3 (2020): 033066.

A comparison of UMAP^[1] clustering using time-series and time–frequency features

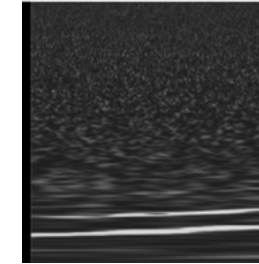
Time-series^[2]



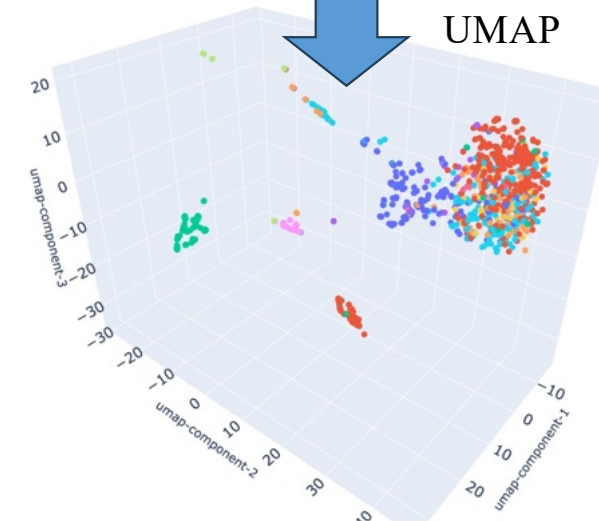
↓ UMAP



Time-Frequency Spectrogram (Q-transform)



↓ UMAP



Note that colors denote different classes of signals.

By visualizing in the upstream process without deep learning, we can obtain a useful benchmark. This at least removes concerns about input data during the tuning phase.

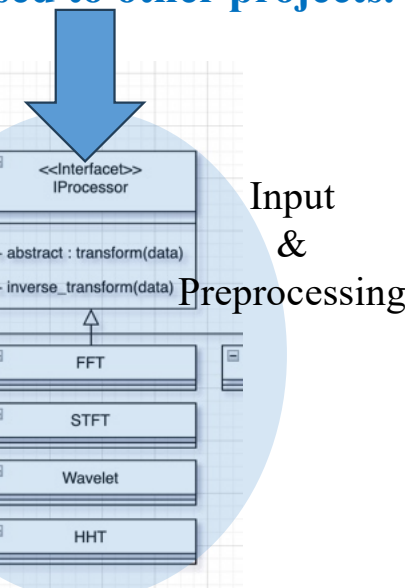
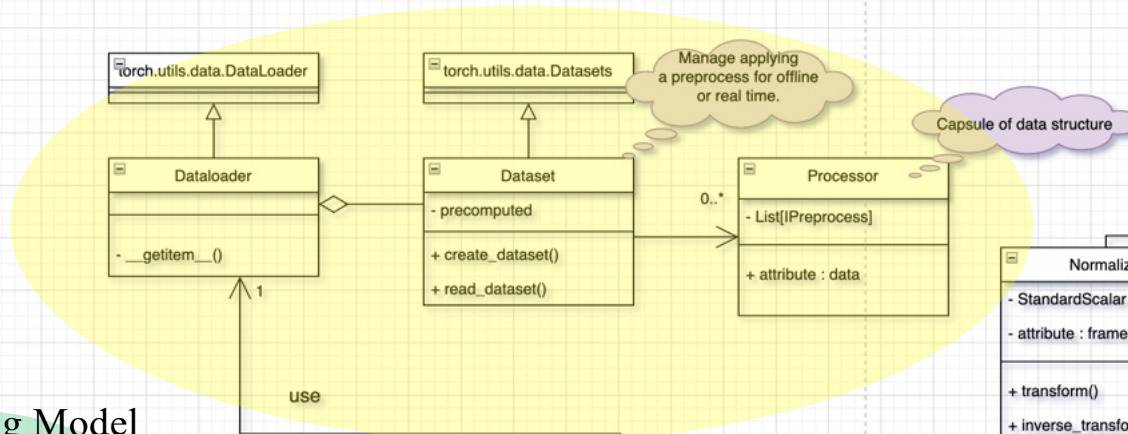
[1] McInnes, Leland, John Healy, and James Melville. *arXiv preprint arXiv:1802.03426* (2018).

[2] <https://www.zooniverse.org/projects/zooniverse/gravity-spy>

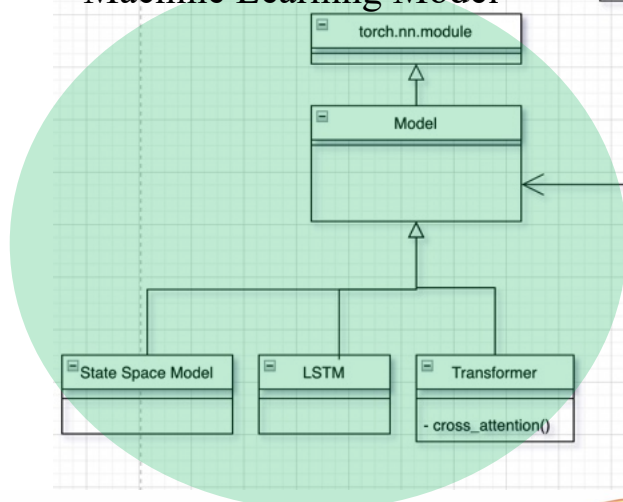
Class Diagram of Machine Learning

Only the input data & preprocessing requires to be implemented
 ✓ **The rest code can be reused to other projects.**

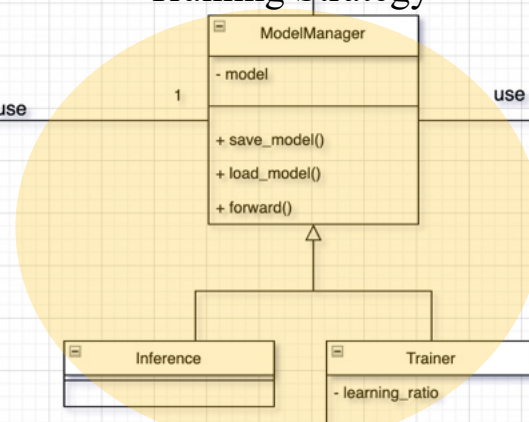
Dataset Configuration



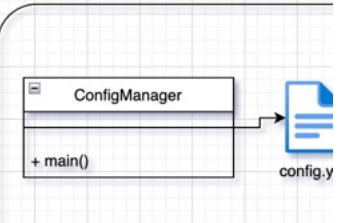
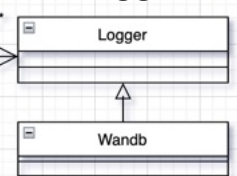
Machine Learning Model



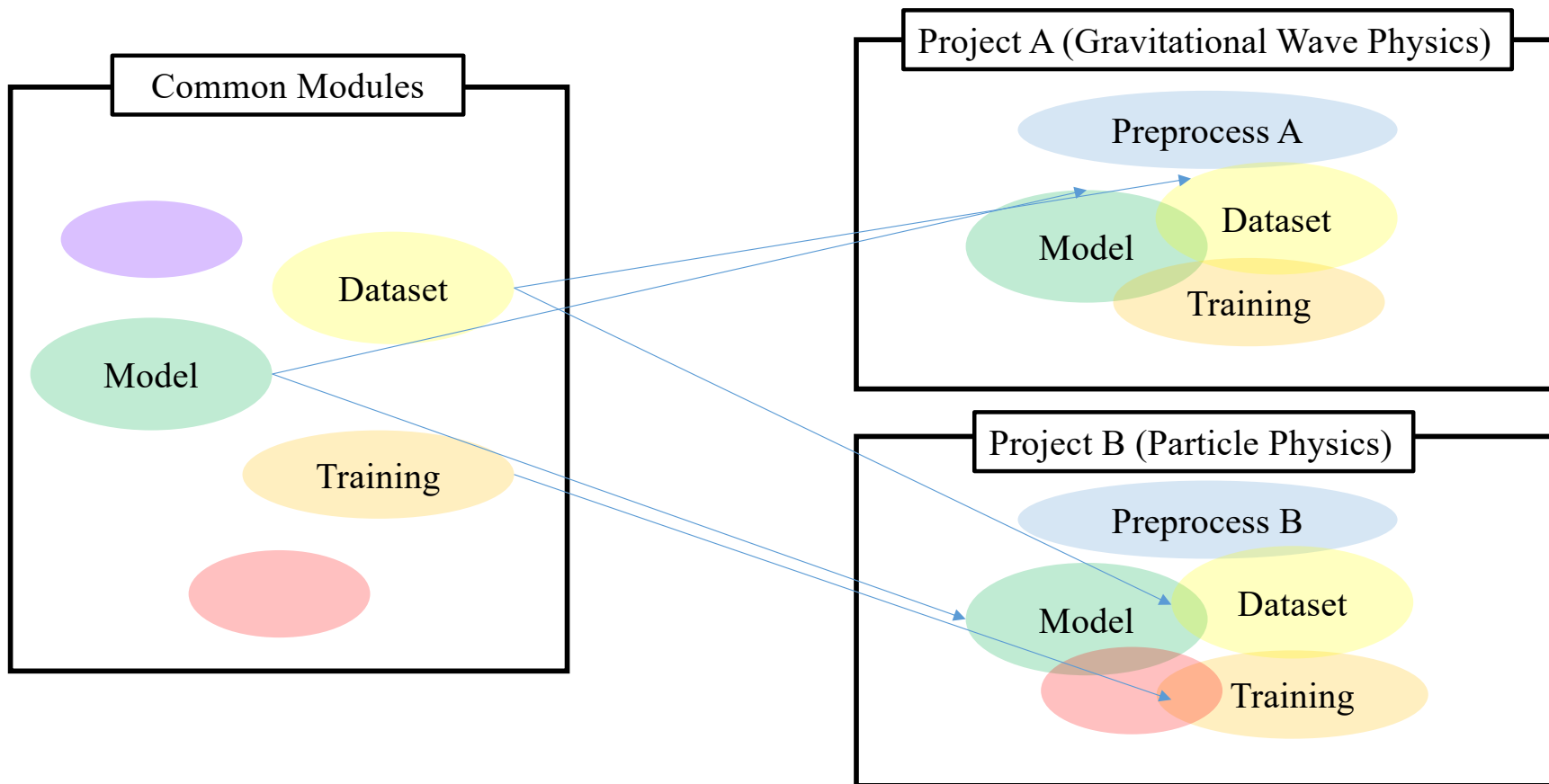
Training Strategy



Logger

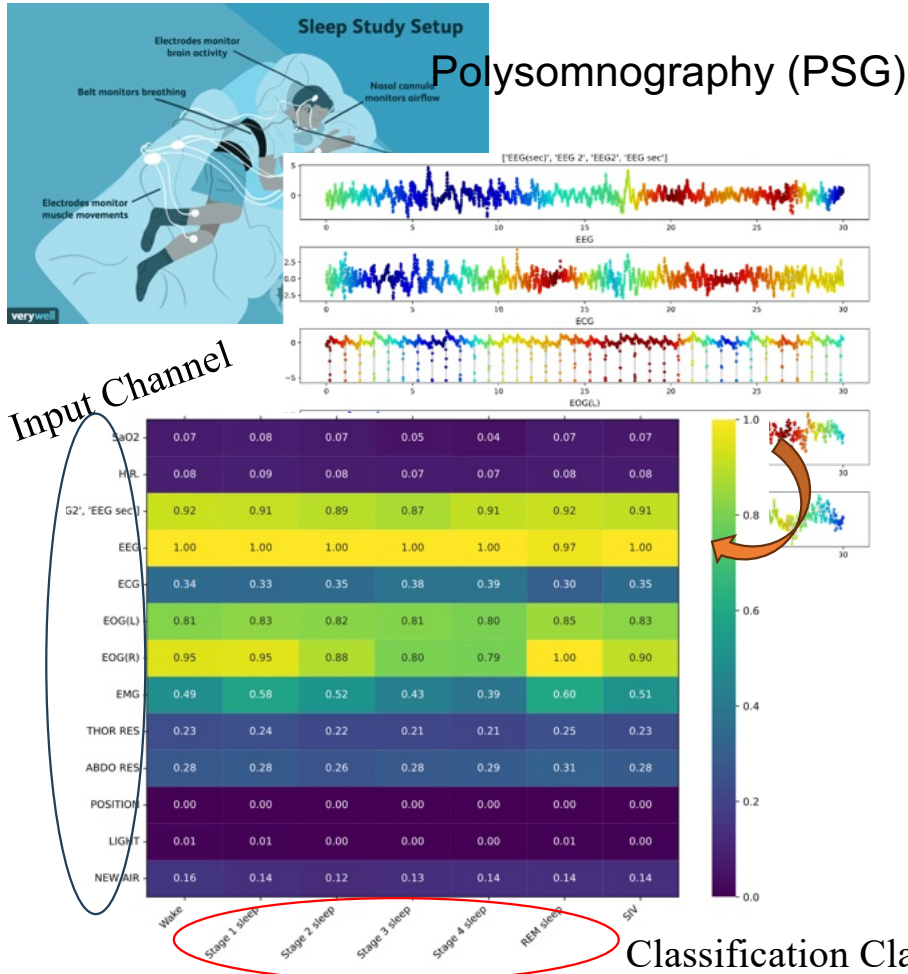


Cross-domain deployment through object-oriented programming

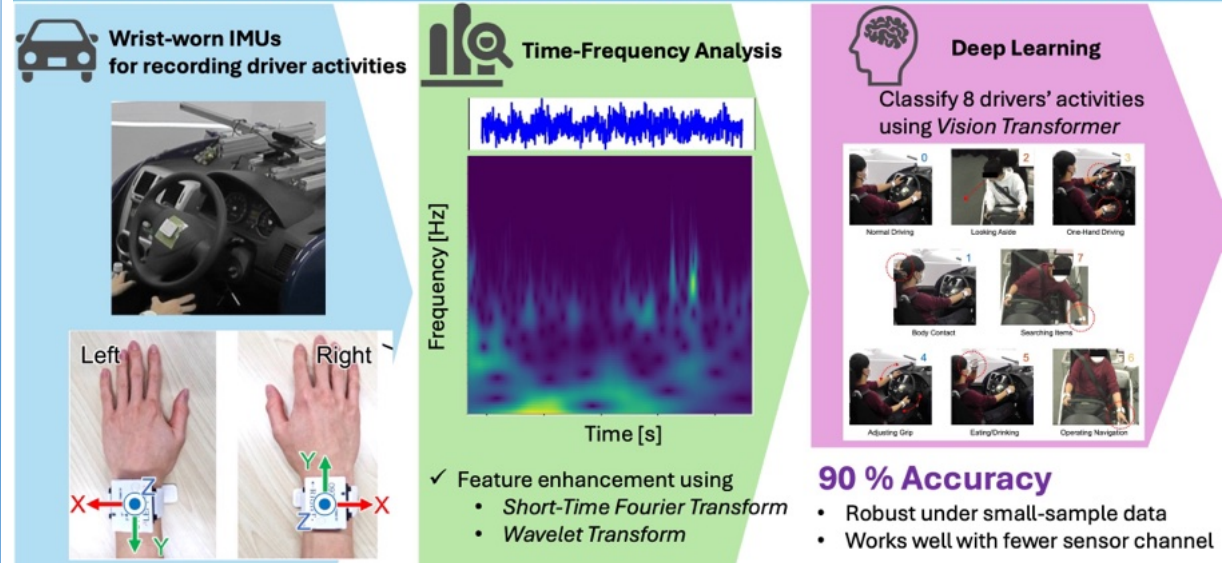


Data Science Studies

Sleep Stage Classification using CNN

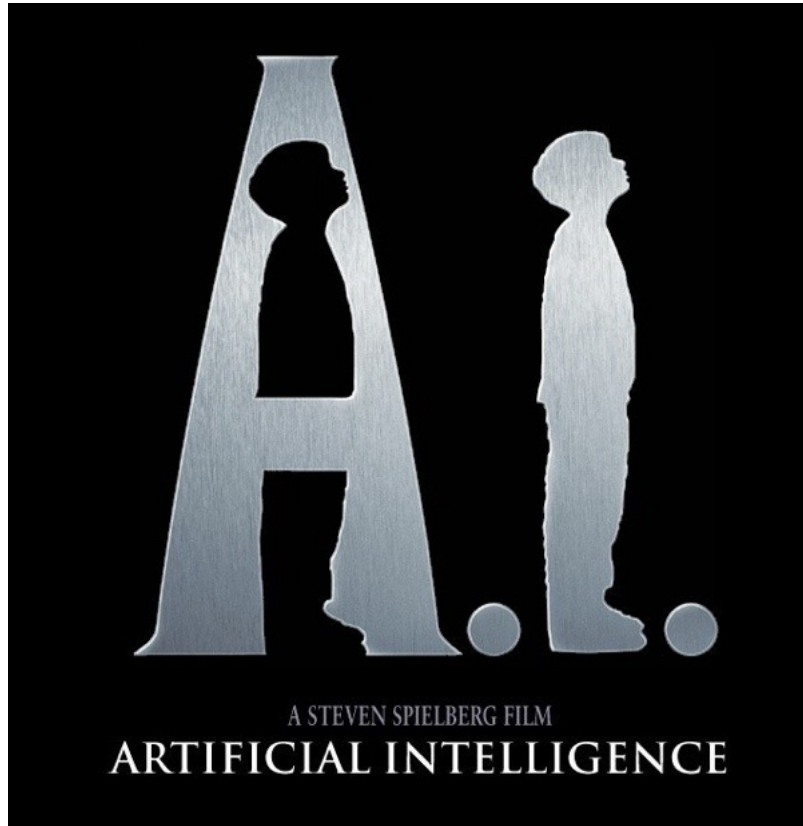


Driver Activity Recognition with Vision Transformer using Time-Frequency Representations Derived from Wrist-Worn Sensors



Y. Sakai, T. Akiduki, M. Meyer-Conde and H. Takahashi, in *IEEE Access*, vol. 13, pp. 188839-188854, 2025, doi: 10.1109/ACCESS.2025.3628273.

Software Design for Machine Learning



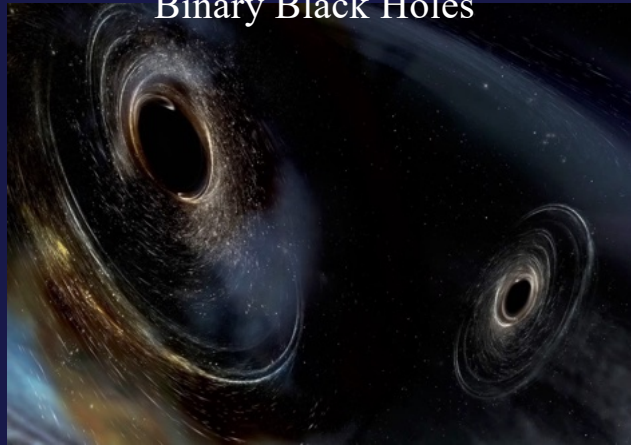
Gravitational-Wave Analysis from Supernova



Types of Gravitational Waves

Modelled

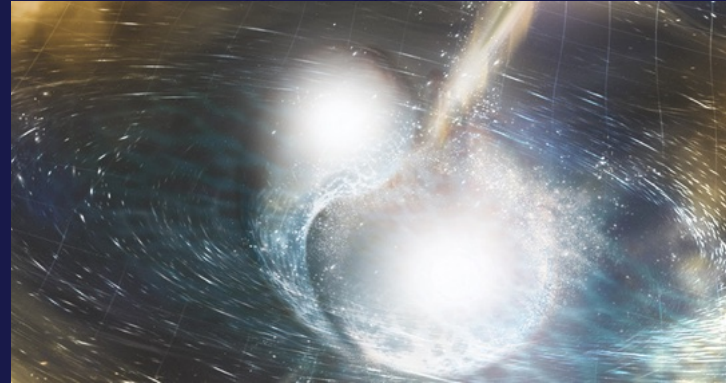
Binary Black Holes



compact binary coalescence



Binary Neutron Stars



continuous



Unmodelled

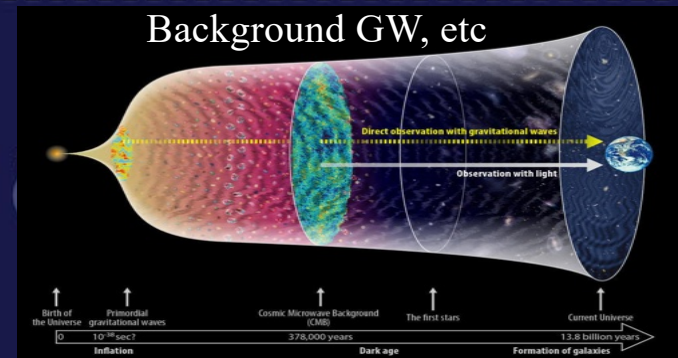
Core-Collapse Supernova



burst



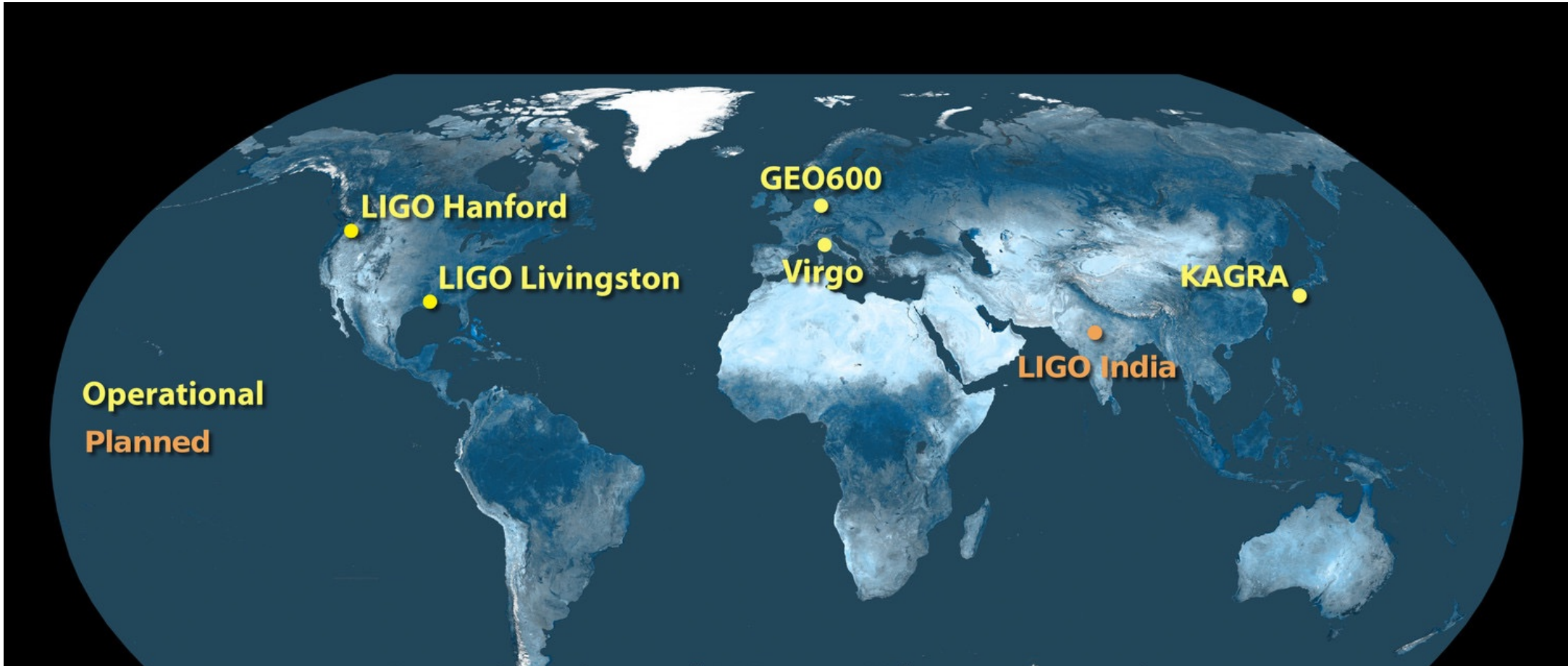
Background GW, etc



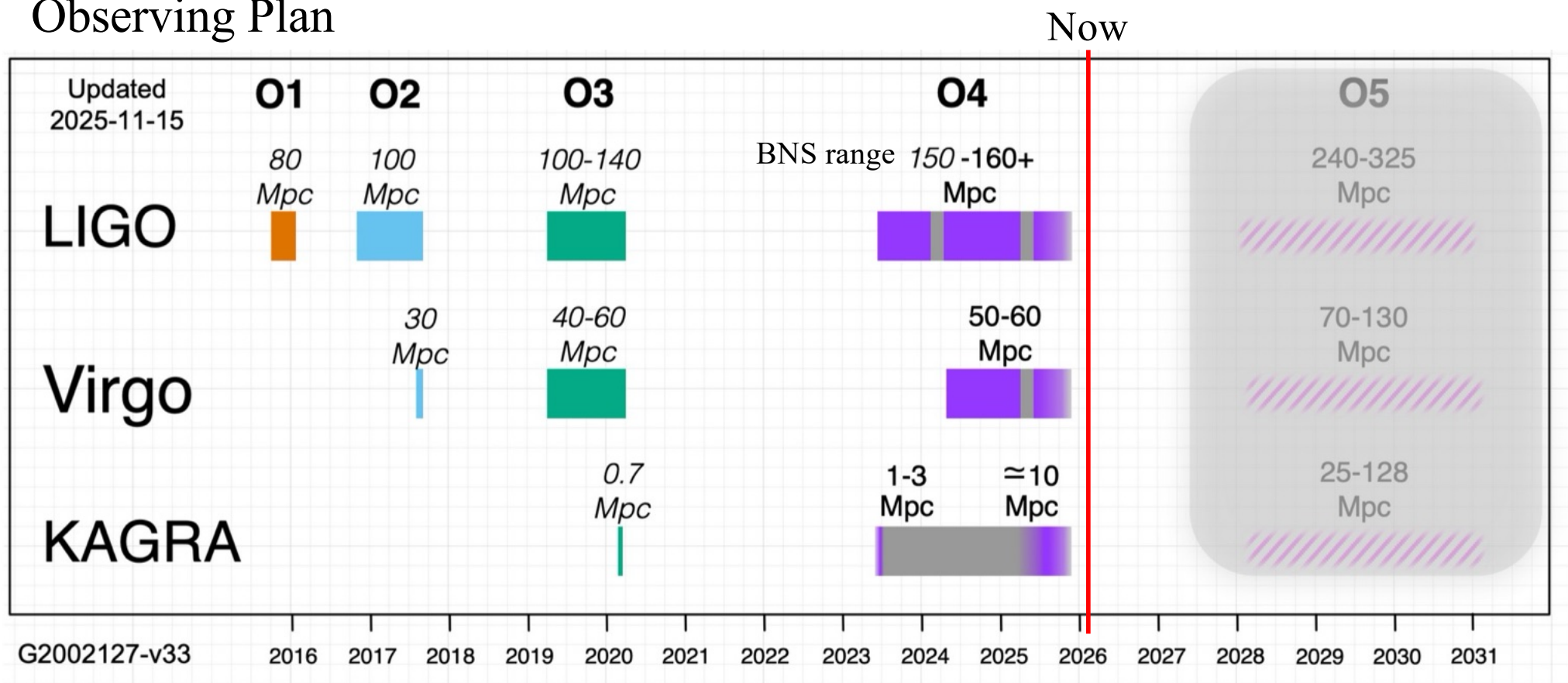
stochastic



The International Gravitational-Wave Observatory Network (IGWN)

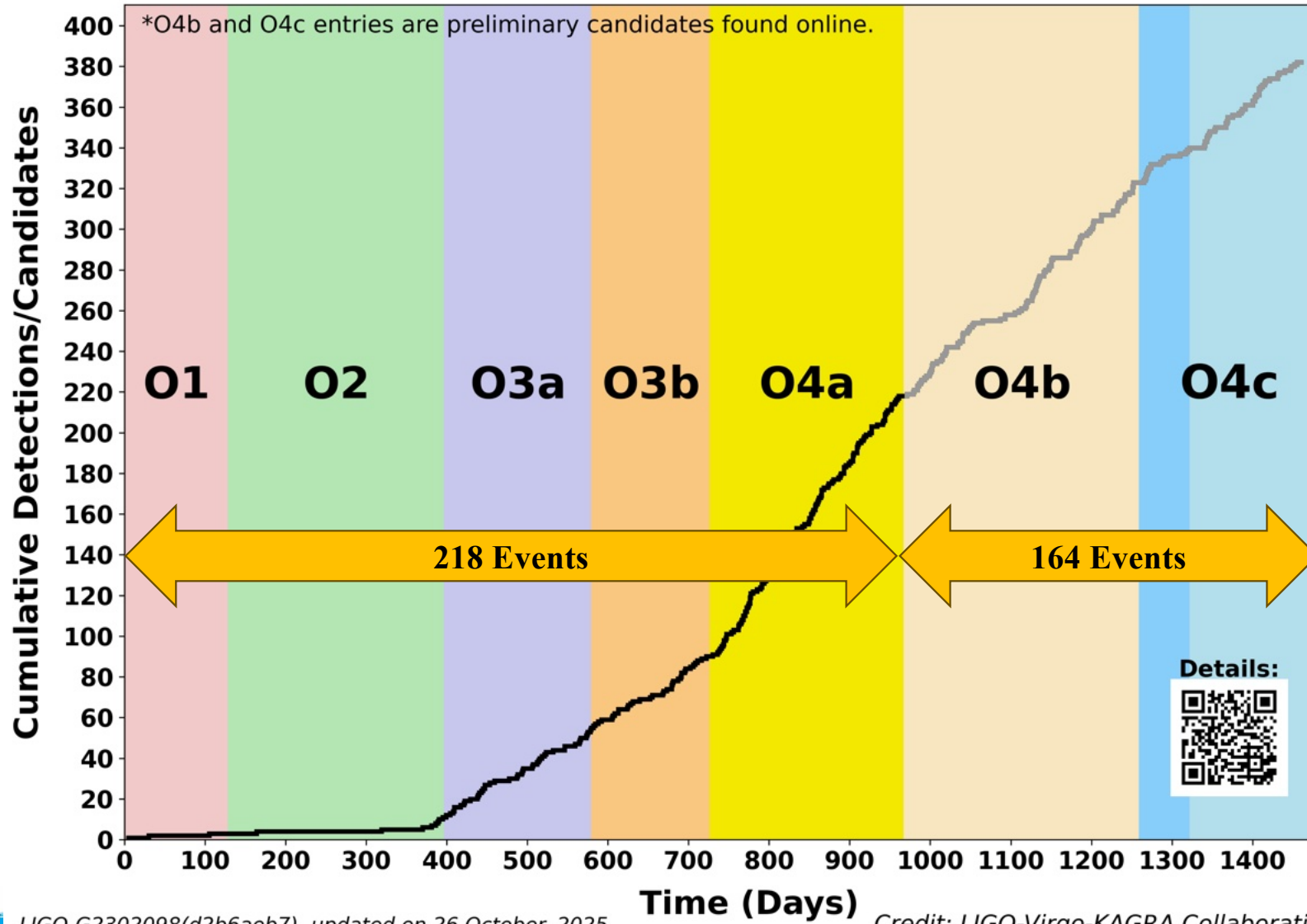


Observing Plan



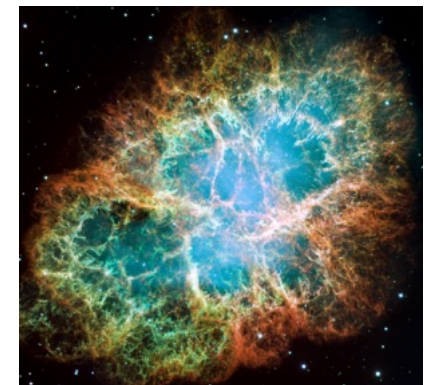
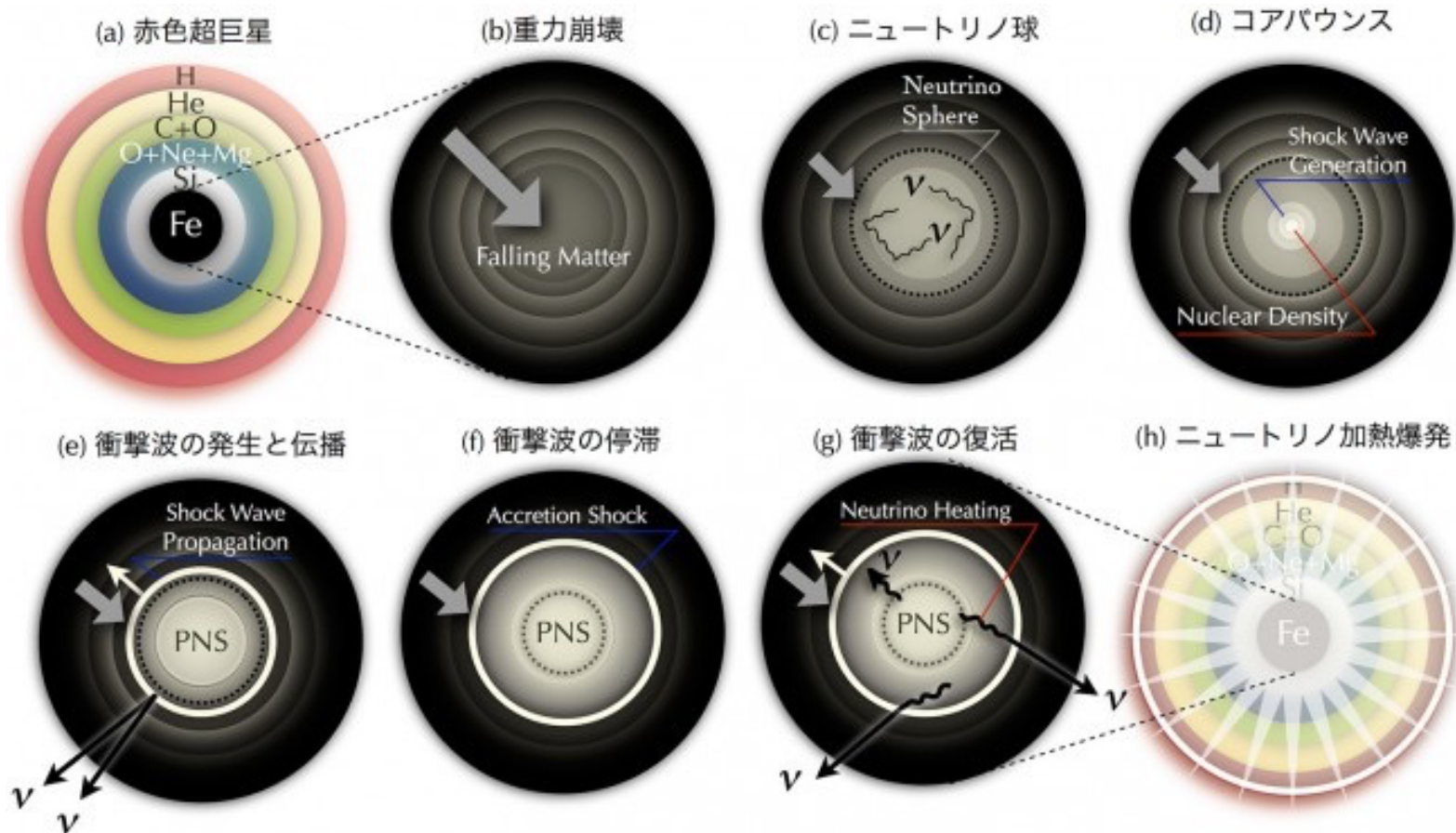
Plans and timeline for the fifth observing run (O5) are being reassessed. Further information will be provided as soon as it becomes available.

O1+O2+O3+O4a = 218, O4b* = 105, O4c* = 59, Total = 382



Scenario of the Core-collapse Supernovae (CCSNe)

Red Giant Star ($M \geq 8M_{\odot}$)



<https://www.jicfus.jp/jp/promotion/pr/mj/2014-3/>

The list of the GWs form 3D CCSNe simulations^[1]

TABLE I. Waveforms from multidimensional CCSN simulations described in the text. For each waveform family we provide a reference, dimensionality, a summary of the numerical method (EOS and code name) and observed GW features. Then, we provide details for example waveforms: identifier, progenitor stellar mass M_{star} , initial central angular velocity Ω_c , the frequency f_{peak} at which the GW energy spectrum peaks, the emitted GW energy E_{GW} and approximate signal duration. The superscript symbols: [†]non-ZAMS, *the simulation was stopped before the full GW signal was developed.

Waveform Family	Numerical Method	GW Features	Waveform Identifier	M_{star} [M_{\odot}]	Ω_c [rad/s]	f_{peak} [Hz]	E_{GW} [$M_{\odot}c^2$]	Duration [ms]
			:					
Powell and Müller 2019, 3D [98]	LS220 CoCoNuT-FMT	g -modes	s3.5_pns	3.5 [†]	...	878	3.6×10^{-9}	700
			s18	18	...	872	1.6×10^{-8}	890
Powell and Müller 2020, 3D [99]	LS220 CoCoNuT-FMT	f -, g -modes SASI prompt-conv.	s18np	18	3.4	742	7.7×10^{-8}	1000
			m39	39	...	674	7.5×10^{-10}	560
			y20	20	...	872	1.0×10^{-8}	980
Radice <i>et al.</i> 2019, 3D [50]	SFHo FORNAX	f -, g -modes SASI/ convection prompt-conv.	s9	9	...	727	1.6×10^{-10}	1100
			s13	13	...	1422	5.9×10^{-9}	800*
			s25	25	...	1132	2.8×10^{-8}	600*

[1] Szczepańczyk, Marek J., et al. *Physical Review D* 104.10 (2021): 102002.

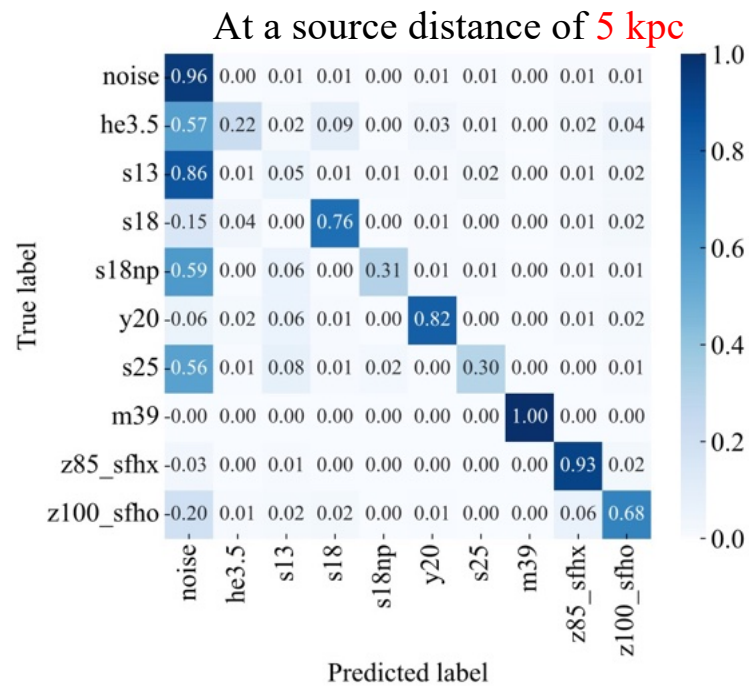
Classification for Gravitational-Waves(GWs) Supernova using CNN

Visualizing Convolutional Neural Network for Classifying Gravitational Waves from Core-Collapse Supernovae

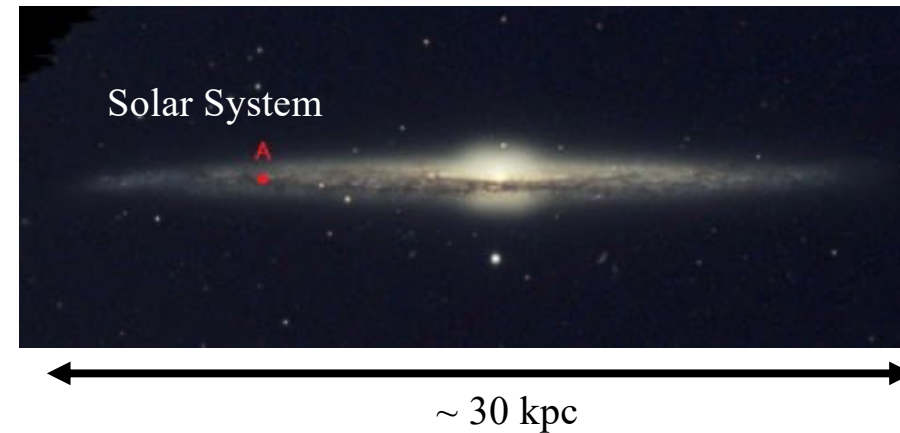
Seiya Sasaoka,¹ Naoki Koyama,² Diego Dominguez,¹ Yusuke Sakai,³
 Kentaro Somiya,¹ Yuto Omae,⁴ and Hirotaka Takahashi^{3,5,6}



GWs represented by short-time Fourier transforms are injected into the LIGO O3 data.

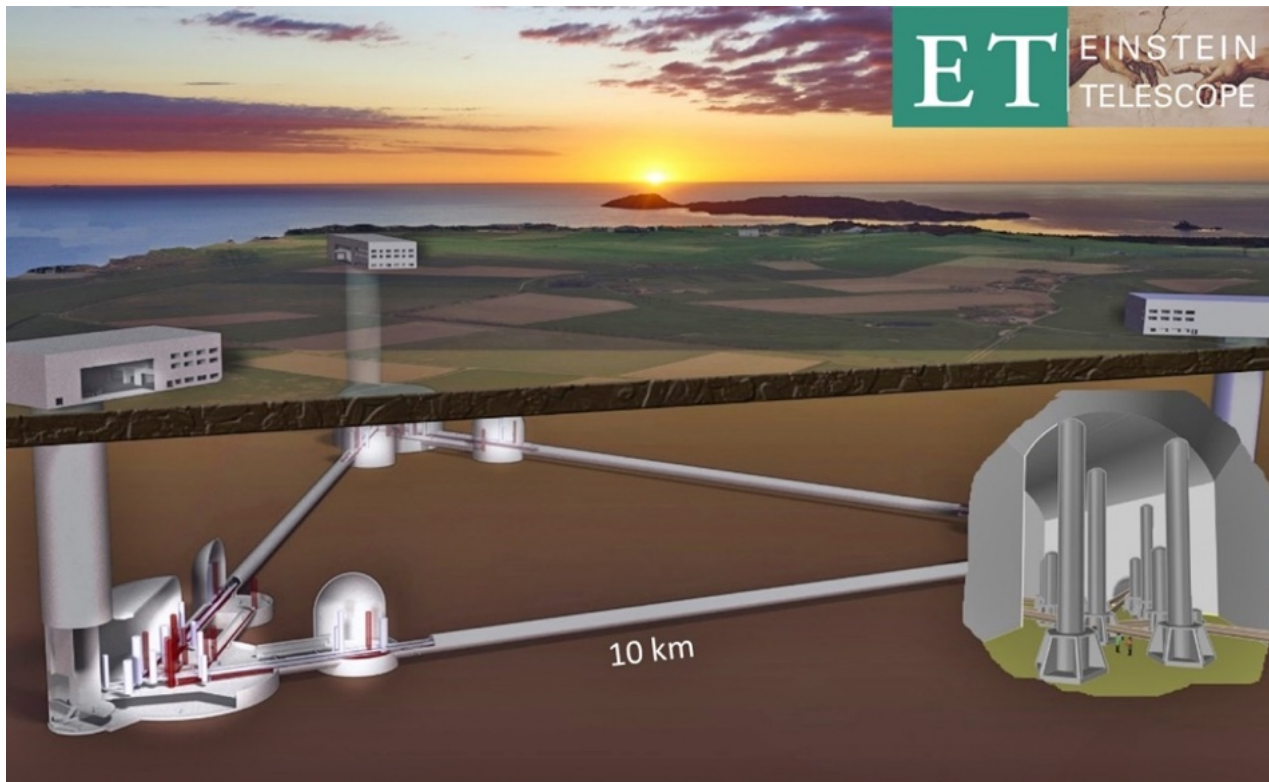


Our Galaxy

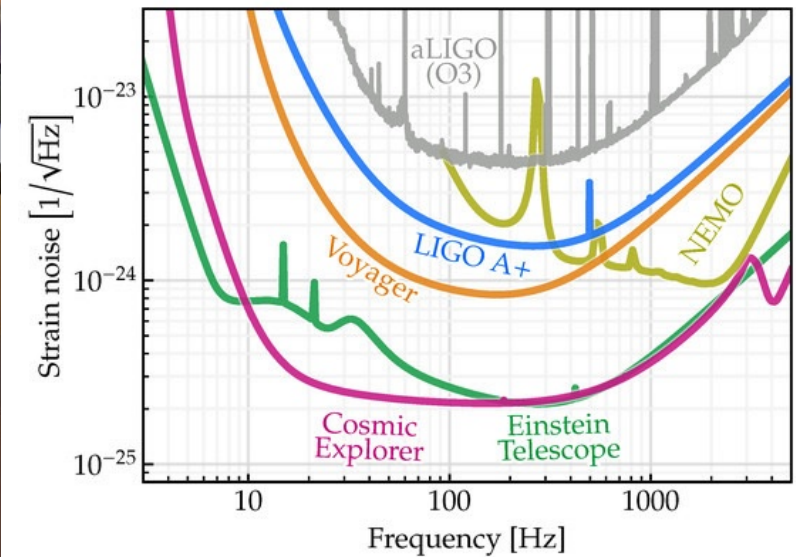


Einstein-Telescope

Next-generation underground observatory designed to detect gravitational waves.



ET will be built in **Europe**.
The construction is planned to start 2028.

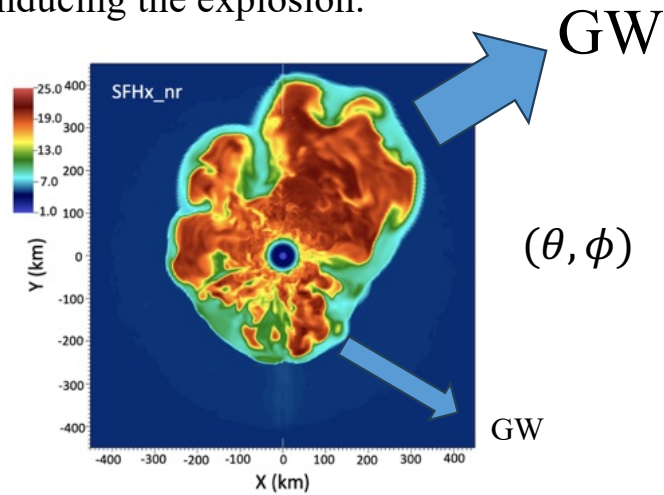


Abac, Adrian, et al. "The science of the Einstein telescope." (2025). arXiv:2503.12263 [gr-qc]

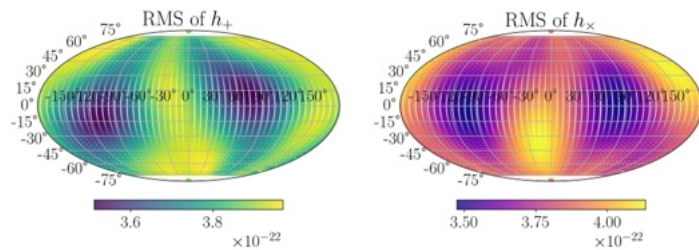


Overview of Our Data Preparation

In CCSNe, asymmetric convection (and instability) within the star is the key to inducing the explosion.



2D meridional slice in the simulation^[1]



7 types of CCSNe

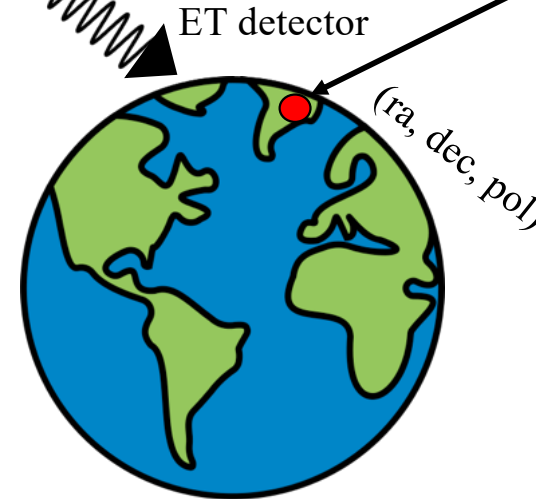
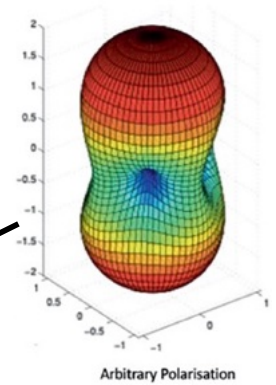


We randomized $(\theta, \phi, ra, dec, pol,)$

Can we identify them?

$$h(t) = F_+(ra, dec, pol, t) h_+(t; \theta, \phi) + F_\times(ra, dec, pol, t) h_\times(t; \theta, \phi)$$

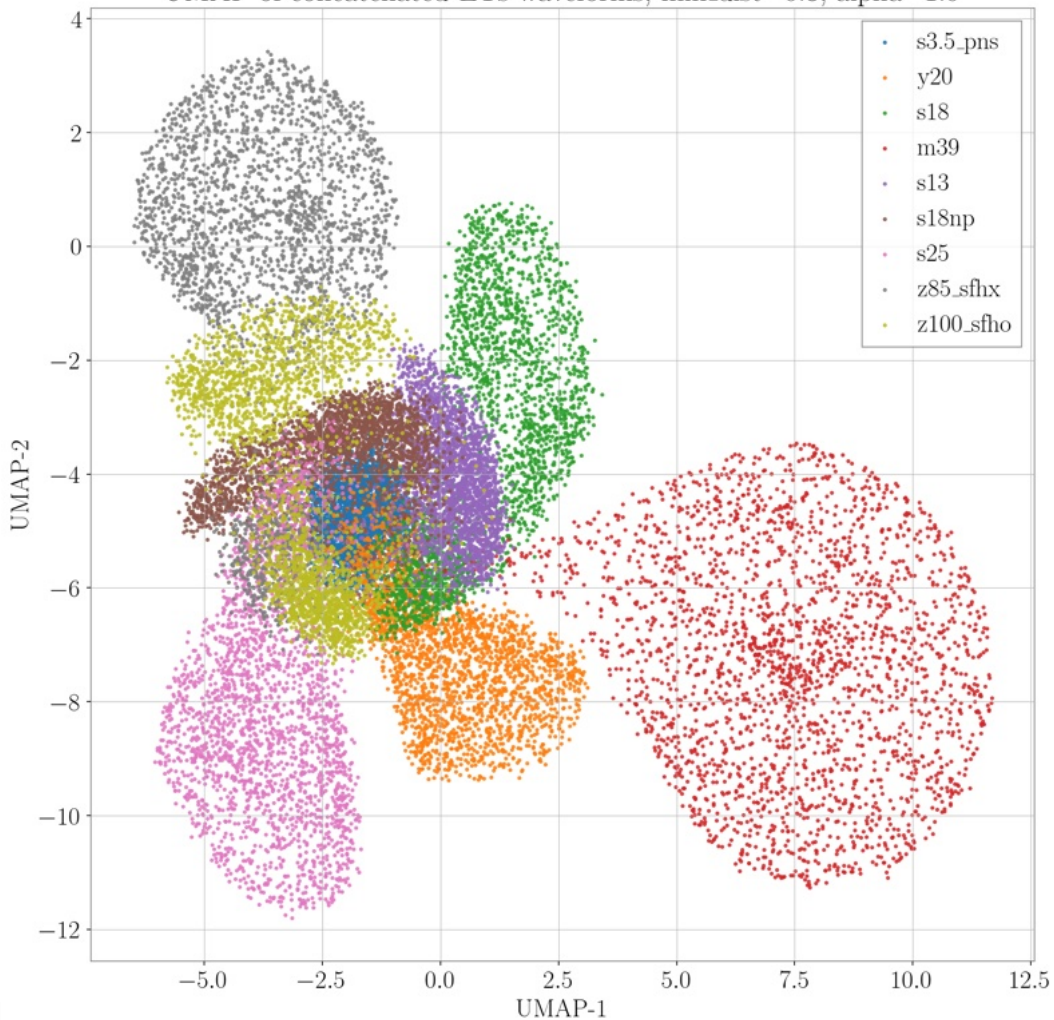
Antenna pattern of a GW detector



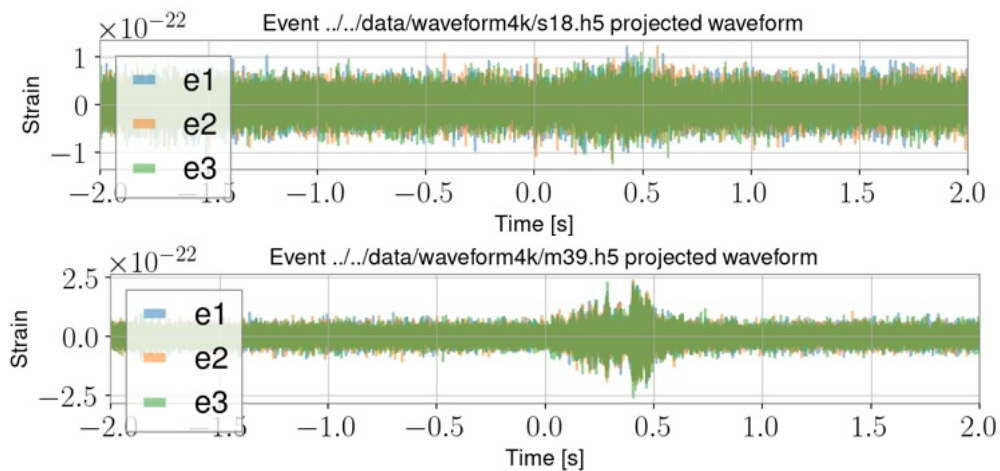
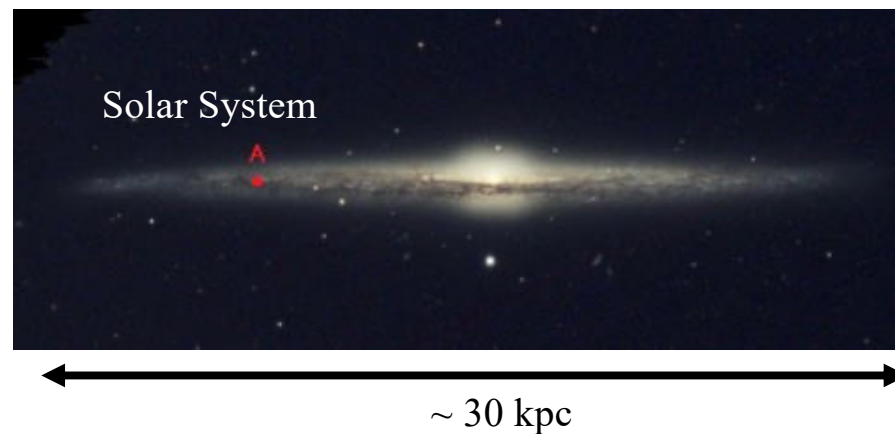
[1] Powell, J., & Müller, B. (2024). *Monthly Notices of the Royal Astronomical Society*, 532(4), 4326-4339.

The source distance at 30kpc

UMAP of concatenated ETs waveforms, min_dist=0.8, alpha=1.0



Our Galaxy

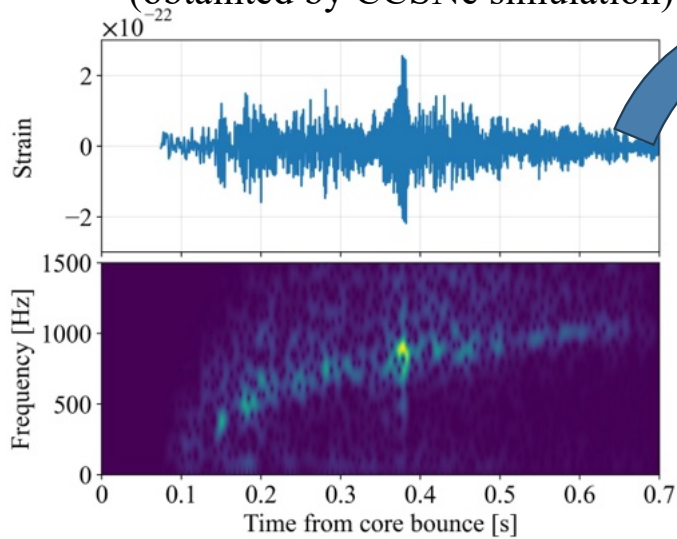


Universal Relations between Gravitational-Wave and Parameters of Proto-Neutron Star

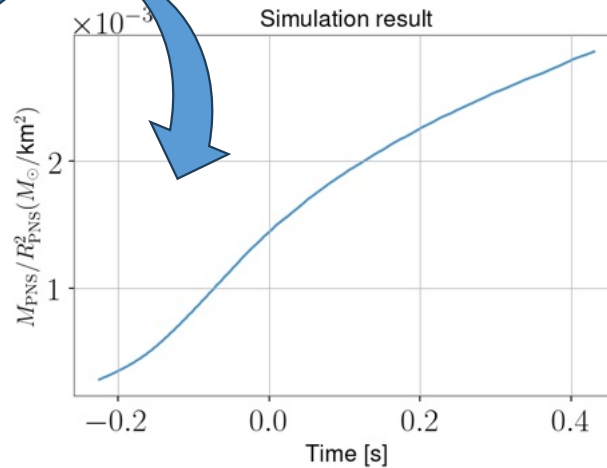
- GWs from CCSNe exhibit characteristic spectrum known as gravitational modes (g-modes), that originate from fundamental fluid oscillations of Proto-neutron star (PNS)^[1].

- Universal relations*^[2]

Gravitational-Wave
(obtained by CCSNe simulation)



$$f_{GW} = f_{\text{universal}} (M_{PNS}/R_{PNS})$$



Representative previous studies:

- Jade Powell and Bernhard Müller, PHYSICAL REVIEW D 105, 063018 (2022)
- H. Sotani, T. Takiwaki, and H. Togashi, Phys. Rev. D 104, 123009 (2021).
- M.-A. Bizouard, P. Maturana-Russel, A. Torres-Forné, M. Obergaulinger, P. Cerdá-Durán, N. Christensen, J. A. Font, and R. Meyer, Phys. Rev. D 103, 063006 (2021).
- T. Bruel, M.-A. Bizouard, M. Obergaulinger, P. Maturana-Russel, A. Torres-Forné, P. Cerdá-Durán, N. Christensen, J. A. Font, and R. Meyer, Phys. Rev. D 107, 083029 (2023)
- A. Casallas-Lagos, J. M. Antelis, C. Moreno, M. Zanolin, A. Mezzacappa, and M. J. Szczepańczyk, Phys. Rev. D 108, 084027 (2023)

Therefore, we can obtain the PNS parameters from the GWs observation!

¹ N. Andersson and K. D. Kokkotas, Mon. Not. R. Astron. Soc. 299, 1059 (1998)

² A. Torres-Forné, P. Cerdá-Durán, M. Obergaulinger, B. Müller, and J. A. Font, Phys. Rev. Lett. 123, 051102 (2019)

Search for Gravitational Waves Emitted from SN 2023ixf



This image from Gemini North shows the supernova SN 2023ixf, located left of center along one of the spiral arms of the galaxy Messier 101. [International Gemini Observatory/NOIRLab/NSF/AURA; CC BY 4.0]

This event was heppend nearby our galaxy.

- ~ 6.4 Mpc (Luminosity Distance)
- SN Type II

THE ASTROPHYSICAL JOURNAL, 985:183 (23pp), 2025 June 1
© 2025. The Author(s). Published by the American Astronomical Society.

<https://doi.org/10.3847/1538-4357/adc681>

OPEN ACCESS



Search for Gravitational Waves Emitted from SN2023ixf

A. G. Abac¹, R. Abbott², I. Abouelfetouh³, F. Acemese^{4,5}, K. Ackley⁶, S. Adhicary⁷, N. Adhikari⁸, R. X. Adhikari², V. K. Adkins⁹, D. Agarwal^{10,11}, M. Agathos¹², M. Aghaei Abchouyeh¹³, O. D. Aguiar¹⁴, I. Aguilar¹⁵, L. Aiello^{16,17,18}, A. Ain¹⁹, T. Akutsu^{20,21}, S. Albanesi^{22,23,24}, R. A. Alfai²⁵, A. Al-Jodah²⁶, C. Alléné²⁷, A. Allocca^{5,28}, S. Al-Shammari¹⁸, P. A. Altin²⁹, S. Alvarez-Lopez³⁰, A. Amato^{31,32}, L. Amez-Droz³³, A. Amorosi³³, C. Amra³⁴, A. Ananyeva², S. B. Anderson², W. G. Anderson², M. Andia³⁵, M. Ando³⁶, T. Andrade³⁷, N. Andres³⁷, M. Andrés-Carcasona³⁸, T. Andric^{1,39,40,41}, J. Anglin⁴², S. Ansoldi^{43,44}, J. M. Antelis⁴⁵, S. Antier⁴⁶, M. Aouim⁴⁷, E. Z. Appavuravther^{48,49}, S. Appert², S. K. Apple⁵⁰, K. Arai², A. Araya³⁶, M. C. Araya², J. S. Areeda⁵¹, L. Argüanas⁵², N. Aritomi³, F. Armato^{33,54}, N. Araud^{35,55}, M. Arogeti⁵⁶, S. M. Aronson⁹, G. Ashton³⁷, Y. Aso^{20,58}

<https://aasnova.org/2025/12/16/selections-from-2025-a-search-for-gravitational-waves-from-sn-2023ixf/>

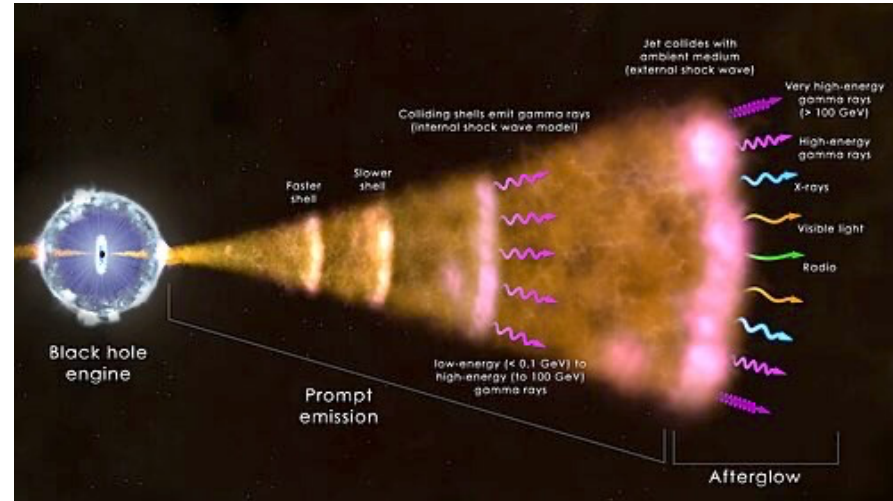
A. G. Abac *et al* 2025 *ApJ* **985** 183 DOI 10.3847/1538-4357/adc681

Assumed time lag between GWs and electromagnetic signals

CCSNe



Gamma-ray bursts



Few seconds \sim few weeks

It's challenging to detect the GWs from these events solely.

- Gravitational-wave and neutrino emissions are expected to rise nearly simultaneously, and their joint observation enhances the detectability of the event.

D. Guetta, D. Hooper, J. Alvarez-Muñiz, F. Halzen, and E. Reuveni, *Astropart. Phys.* 20, 429 (2004)

Ott, Christian D., et al. " *Nuclear Physics B-Proceedings Supplements* 235 (2013): 381-387.

S. S. Kimura, K. Murase, P. Mészáros, and K. Kiuchi, *ApJ* 848, L4 (2017).

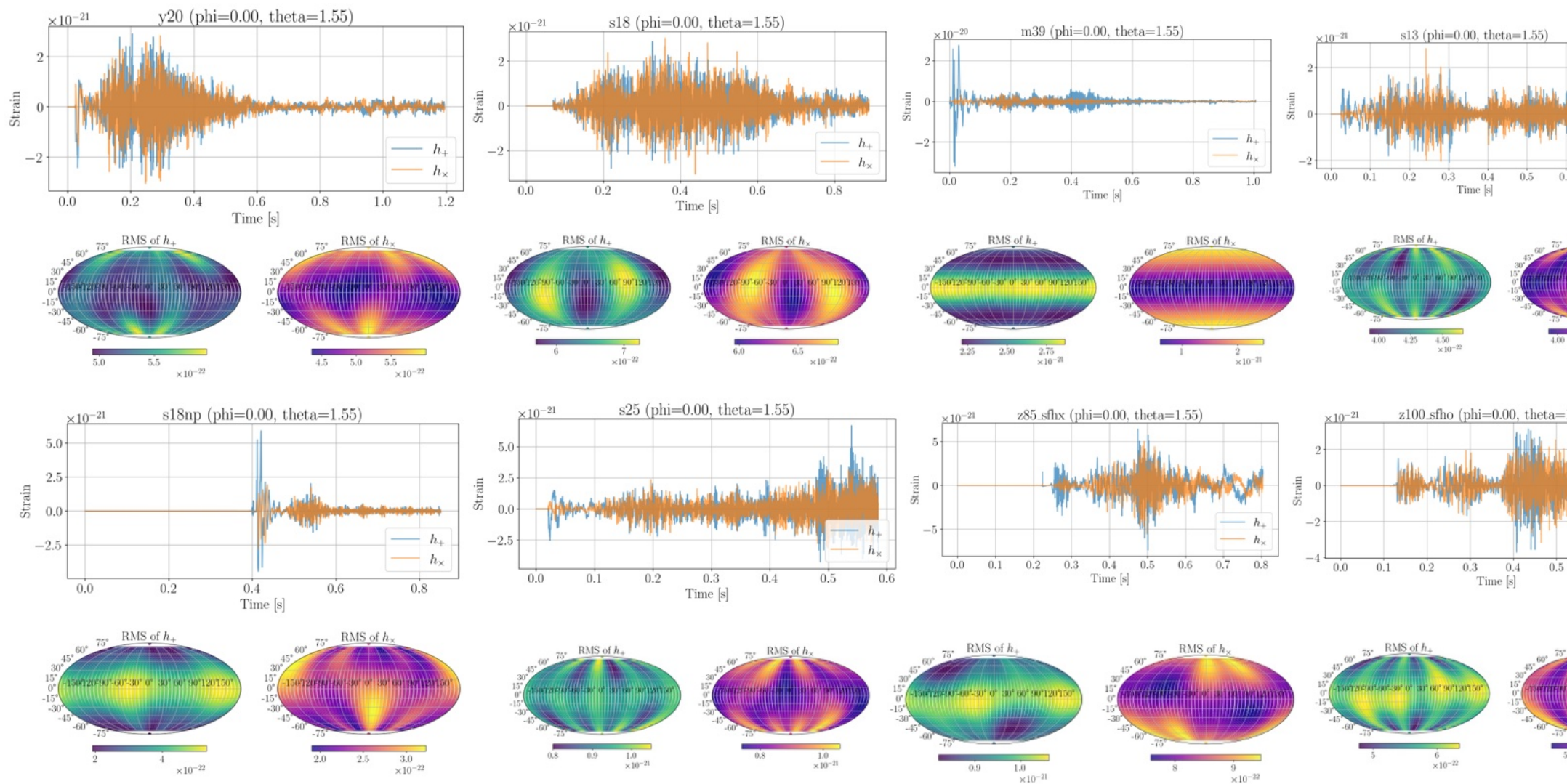
Conclusion

- Even though our research fields differ, sharing common knowledge in machine learning should allow us to mutually accelerate our research.
- Further progress in physics is expected through future gravitational-wave detection from core-collapse supernovae.



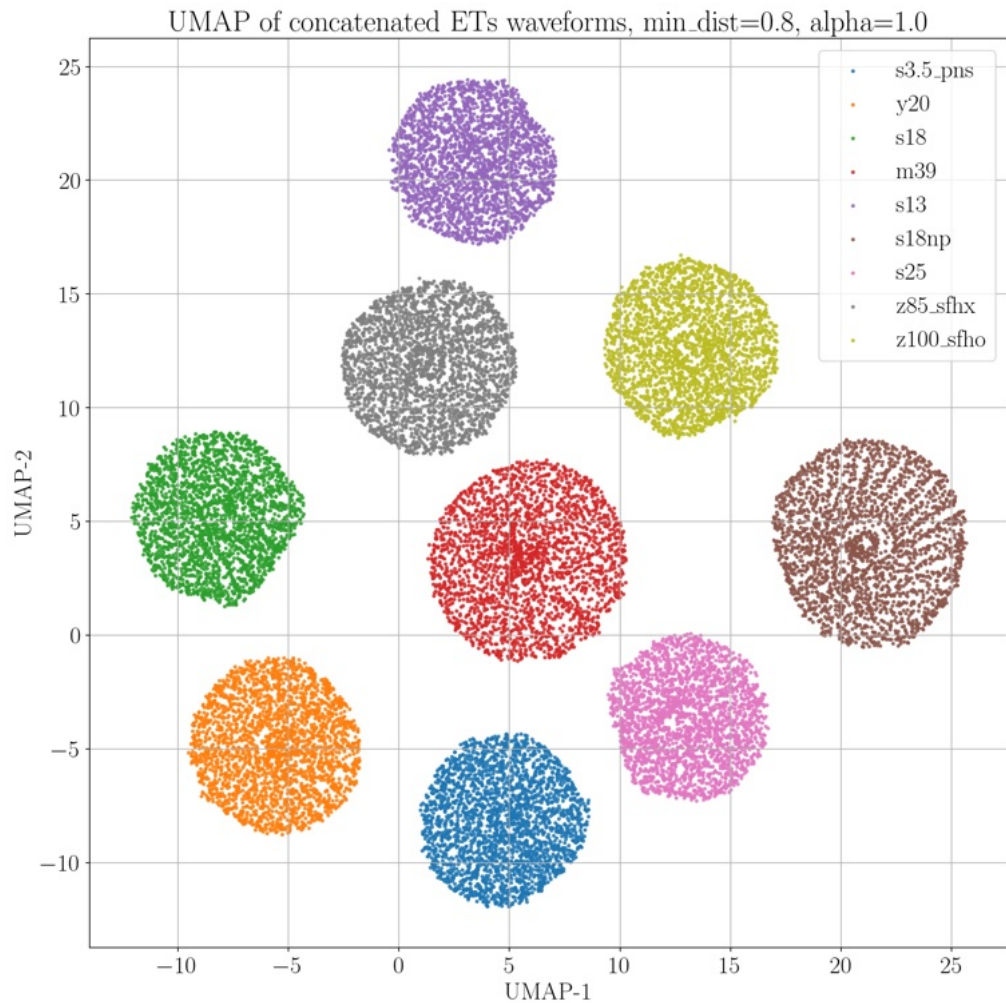
Appendix



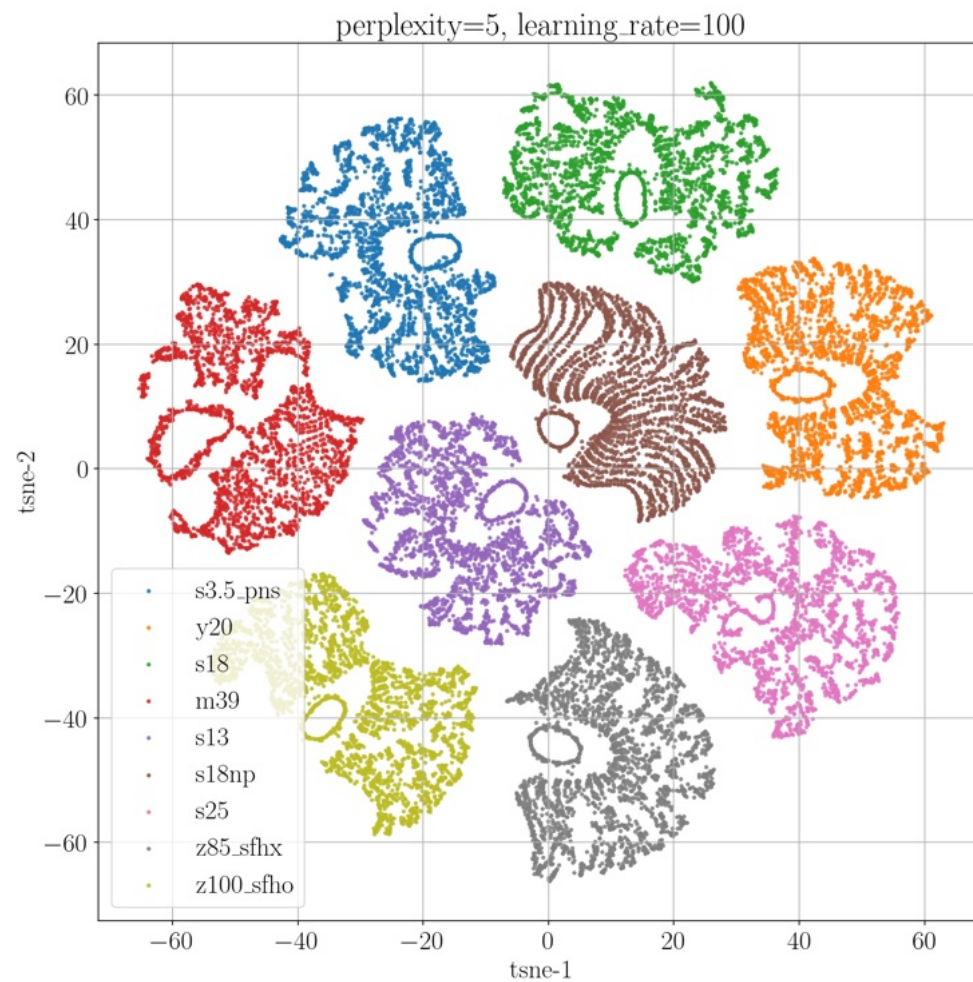


Non-noise Condition

UMAP



t-SNE



Universal Relations

PHYSICAL REVIEW LETTERS **127**, 239901(E) (2021)

TABLE I. Parameters of the universal relations found for each of the modes considered. Fits are of the form $f = a + bx + cx^2 + dx^3$, with f expressed in hertz, and using M_{\odot} and kilometers as units for mass and length in the quantities expressed in the variable x . Note that some coefficients are not used in some fits. R^2 and σ are the correlation coefficient and the standard deviation of the data (in hertz) with respect to the fit, respectively.

Mode	x	a	$b/10^5$	$c/10^6$	$d/10^9$	R^2	σ
2f	$\sqrt{M_{\text{shock}}/R_{\text{shock}}^3}$...	1.410 ± 0.004	-4.23 ± 0.06	...	0.966	45
2p_1	$\sqrt{M_{\text{shock}}/R_{\text{shock}}^3}$...	2.205 ± 0.007	4.63 ± 0.09	...	0.991	61
2p_2	$\sqrt{M_{\text{shock}}/R_{\text{shock}}^3}$...	4.02 ± 0.02	7.4 ± 0.3	...	0.983	123
2p_3	$\sqrt{M_{\text{shock}}/R_{\text{shock}}^3}$...	6.21 ± 0.03	-1.9 ± 0.6	...	0.979	142
2g_1	$M_{\text{PNS}}/R_{\text{PNS}}^2$...	8.67 ± 0.03	-51.9 ± 0.5	...	0.958	205
2g_2	$M_{\text{PNS}}/R_{\text{PNS}}^2$...	5.88 ± 0.03	-86.2 ± 1.0	4.67 ± 0.08	0.956	85
2g_3	$\sqrt{M_{\text{shock}}/R_{\text{shock}}^3} p_C / \rho_C^{2.5}$	905 ± 3	-79.9 ± 1.7	-11000 ± 2000	...	0.925	41